

Optical and photophysical properties of Ag/CdS nanocomposites—An analysis of relaxation kinetics of the charge carriers

Anil Kumar*, Vidhi Chaudhary

Department of Chemistry and Centre of Nanotechnology, Indian Institute of Technology Roorkee, Roorkee 247667, India

Received 30 October 2006; received in revised form 8 February 2007; accepted 10 February 2007

Available online 22 February 2007

Abstract

Ag/CdS nanocomposites have been synthesized and characterized by TEM, XRD, electronic and fluorescence spectroscopy. The content of Ag modifies the nature of surface interaction between the two components as revealed by TEM, electronic and fluorescence measurements. Increasing contents of silver in the composite reduces the interparticle separation. The addition of silver blue shifts the absorption maxima and, influences the emission behavior and charge dynamics in a complex manner. At low molar ratio of Ag:CdS about five-fold enhancement in fluorescence is observed which is attributed to the excited state charge transfer interaction between the two components. On the contrary at high Ag the fluorescence intensity is reduced significantly to become smaller than that of pure CdS nanoparticles. The quenching of emission is understood to occur by the rapid electron transfer from the excited CdS to Ag particle. Relaxation kinetics of charge carriers of CdS also reveal the formation of transitory CT complex between excited CdS and Ag, in which the extent of electron transfer is controlled by the amount of Ag and thus supporting the steady-state findings. A mechanism of these processes is discussed.

© 2007 Elsevier B.V. All rights reserved.

Keywords: Nanocomposite; Ag/CdS; Fluorescence; Optical; Charge carriers dynamics

1. Introduction

Nanoscale composites comprising surface modified metals, semiconductors, and metal–semiconductor are being synthesized in order to fabricate tailored materials with tunable electronic and photonic properties [1–4]. A change in their physicochemical properties can be anticipated due to the combined effect of different components as regards to their size, enhanced interface and surface interaction. In recent years metal–semiconductor nanocomposites have been studied extensively because of their characteristic optical, emission and non-linear optical behavior [5–9], photocatalytic effect [2], varied charge dynamics [10], surface enhanced Raman scattering (SERS) effect [10–12], etc. as these aspects may find potential applications in photocatalysis and the fabrication of devices.

Metal–semiconductor assemblies comprising colloidal particles are interesting because of a weak van der Waals interaction between the two phases, which might be expected to have

several beneficial effects in terms of their organization, increased interface, improved charge carrier dynamics, reactivity and selectivity. A number of synthetic approaches have been used to obtain nanoscale composites viz. by reduction of metal ion(s) on semiconductors [13,14], producing them in a core shell structure [15,16], and through electrostatic interaction using charged colloidal particles [10,17], etc. Several reports on these systems have focused on the investigation of their optical properties because of the local field enhancements in the presence of metals [5–8]. As regard to their fluorescence behavior, we have come across a few reports on colloidal Ag/CdTe [10], Au/CdS [18], CdTe nanocrystal spin coated in PVA matrix on glass and silver island films [19] and biconjugates of Au nanoparticles with CdTe nanowires in solution [8]. In the first two cases an increase in molar ratio of metal to semiconductor results in the quenching of emission due to the semiconductor component, whereas in the latter reports an enhancement of luminescence was observed.

In the present work we have investigated optical and fluorescence behavior of Ag/CdS nanocomposites prepared from its colloidal components in aqueous medium. Steady-state optical, fluorescence and time-resolved fluorescence techniques have been used to analyze the interaction between the two phases

* Corresponding author. Tel.: +91 1332 285799; fax: +91 1332 273560.
E-mail address: anilkfcy@iitr.ernet.in (A. Kumar).

and the dynamics of charge carriers in the irradiated system. In the composite Ag and CdS phases have been identified by TEM, XRD, electronic, and fluorescence spectroscopy. Interestingly, at low molar ratios of Ag to CdS, an increase in their ratio up to 0.25 results in the enhancement of fluorescence intensity and, thereafter, any further increase causes the quenching of emission. Under the used experimental conditions steady-state observations could be correlated to the time-resolved measurements. A mechanism of the occurring processes has been worked out.

2. Experimental

2.1. Reagents

Cadmium perchlorate, dialysis membrane (Aldrich); sodium hexametaphosphate, hydrochloric acid (Qualigens); sodium citrate tribasic dihydrate (SRL); silver nitrate, sodium hydroxide, perchloric acid (Merck); N₂ having purity >99.9% (Sigma) were of analytical grade and were used as received without further purification. Silver nanoparticles were dialyzed by using spectra/por membrane (M.W. 6000–8000).

2.2. Equipment

Electronic spectra were measured on a Shimadzu UV2100S spectrophotometer. Steady-state emission measurements were made on a Shimadzu RF-5301PC spectrofluorophotometer. Electron micrographs and selected area diffraction patterns were recorded on a Philips EM-400 transmission electron microscope equipped with image analysis system having variable magnifications up to 80,000 \times . X-ray diffraction patterns were recorded on a Philips DW 1140/90 X-ray diffractometer using Cu K α line of the X-ray source. Photolysis of different semiconductor systems were carried out on an Oriel photolysis assembly equipped with stand alone ignitor and a 200 W mercury-xenon lamp. Reaction samples were photolyzed using UG 340 band pass filter. Elimination of all other radiation below and above this range of wavelengths was further ensured by using additional solution filters. The fluorescence lifetimes were measured on a Horiba Jobin Yvon Fluorescence Lifetime System using NanoLEDs and LDs as excitation sources. Solid samples of Ag/CdS nanocomposites were prepared by removing water on a Buchi Rotavapor R111H.

2.3. Methodology

Preparation of colloidal silver: Silver nanoparticles were prepared by following Turkevich method [20], in which aqueous silver nitrate is reduced by sodium citrate solution, which also acted as a stabilizer. Sodium citrate was added drop wise to the silver nitrate solution, the resulting solution was kept boiling for about 40 min, which depicted greenish yellow tinge. The amount of the citrate and the boiling time of the solution were optimized by monitoring the absorbance of the colloidal solution at 420 nm upon varying the concentration of sodium citrate and the boiling time required for the completion of reduction.

The minimum molar ratio of Ag⁺ to citrate and the time of boiling were found to be 1:1 and 40 min, respectively. To ensure the removal of excess citrate and silver ions; the resulting colloidal solution was dialyzed overnight. The absorbance of the resulting Ag nanoparticles by this method was found to be similar to that prepared by γ -radiolysis method [21].

Colloidal CdS solution was prepared using previously reported literature method [22a] by adding 7.5×10^{-5} mol dm⁻³ of freshly prepared SH⁻ to the deaerated 1×10^{-4} mol dm⁻³ aqueous Cd(ClO₄)₂ containing HMP 5×10^{-5} mol dm⁻³ at pH 10.5.

Preparation of Ag/CdS nanocomposite: Ag/CdS nanocomposites were synthesized by adding colloidal solution of Ag to the Cd²⁺ solution prior to the precipitation of CdS [22b], as well as by simple mixing of the two colloidal solutions prepared separately by varying the molar ratio of Ag to CdS nanoparticles from 0.1 to 1.

Transmission electron micrographs of different colloids were recorded by applying a small drop of colloidal solution to carbon coated copper G-200 grid. Copper grid was dried in the dark prior to its examination. The particle size was measured using soft imaging system from GmbH, Germany. Fluorescence decay curves were analyzed kinetically by DAS6 software from IBH. The goodness of the fit was determined by evaluating χ^2 from the fitted plots.

3. Results

Electronic spectra of Ag/CdS nanocomposites, prepared by adding varied amount Ag nanoparticles prior to the precipitation of CdS, have been depicted in Fig. 1a–d. Each of these figures exhibit spectra recorded immediately after preparation, upon aging of this solution and simple additive spectra of its two components. At low molar ratios of silver nanoparticles (up to 0.25), the electronic spectra of fresh and aged samples were very similar but at higher molar ratios, the aged samples depicted less absorption in the entire visible range. A comparison of the absorption spectra of aged samples to those with their simple sum spectra reveal that the electronic spectra of aged samples exhibited relatively less absorption in the entire recorded wavelength range along with a blue shift in the absorption maxima.

Fig. 2 presents the electron micrographs of colloidal silver, CdS, and their nanocomposites containing different molar ratio of Ag:CdS (0.1, 0.25 and 1.0). Silver and CdS particles are produced with an average size of 16 nm and 5 nm, respectively. A careful examination of electron micrographs of composite particles reveals that an increasing amount of silver in the composite influences the nature of micrograph. At low concentrations of silver, Ag particles are surrounded by CdS and remain fairly separated to each other. At mild concentrations of Ag the formation of clusters starts, whereas at its higher concentrations CdS particles are produced at the interface of Ag particles, and these particles grew to form a chain like system.

The selected area diffraction patterns (SAED) for colloidal Ag, CdS and their composite having molar ratio of Ag:CdS of 0.1 are shown in Fig. 3. An analysis of the d value and the indexing of

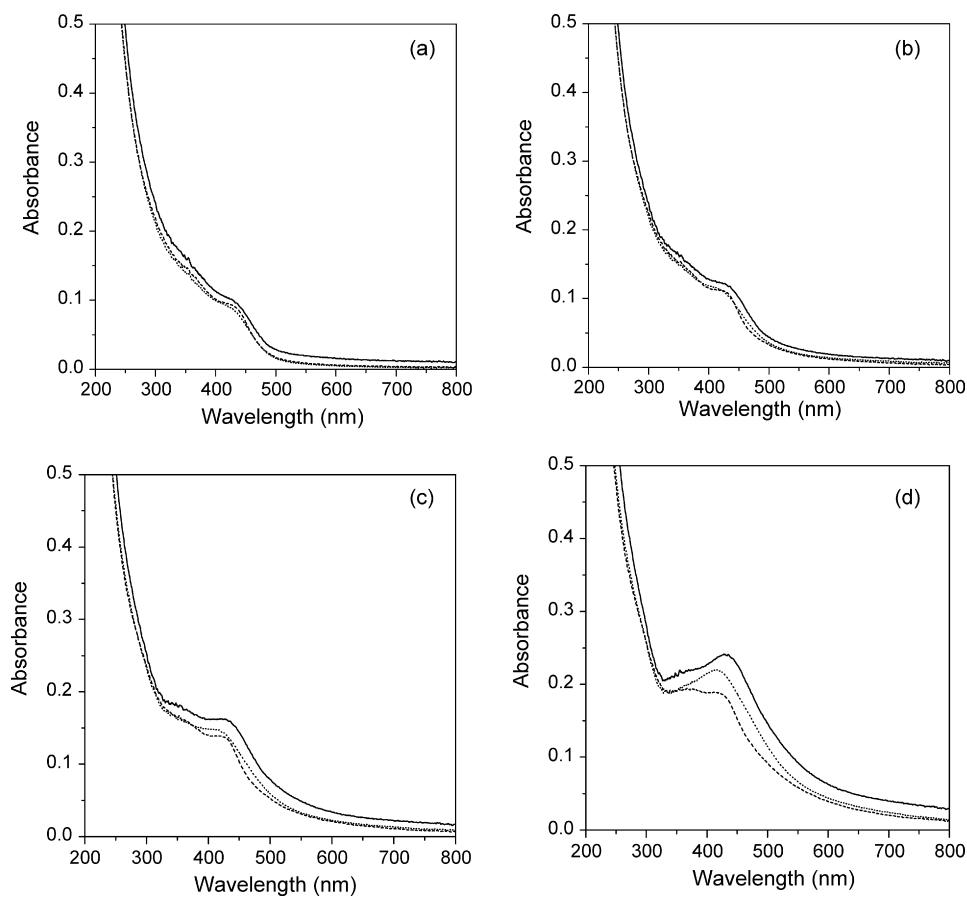


Fig. 1. Electronic spectra of Ag–CdS composite containing varied molar ratio of Ag to CdS: 0.1 (a); 0.25 (b); 0.5 (c); 1 (d). Different curves shown in the above figure: sum spectra (—); fresh sample (..); aged sample (---).

the rings in SAED pattern (Fig. 3c) shows that CdS [2.06 (1 1 0), 1.67 (0 0 4), 1.34 (2 1 0), 1.03 (2 2 0)] and Ag [1.66 (0 0 6), 1.38 (1 1 2), 1.17 (2 0 3), 1.00 (0 0 1 0)] in the composite are of crystalline nature, and each of these are present in hexagonal phase,

respectively. To further confirm the structure of CdS and silver phases in the composite, its X-rays diffraction pattern was also recorded (Fig. 3d) and the diffraction data is summarized in Table 1. The observed values of d -spacing clearly support

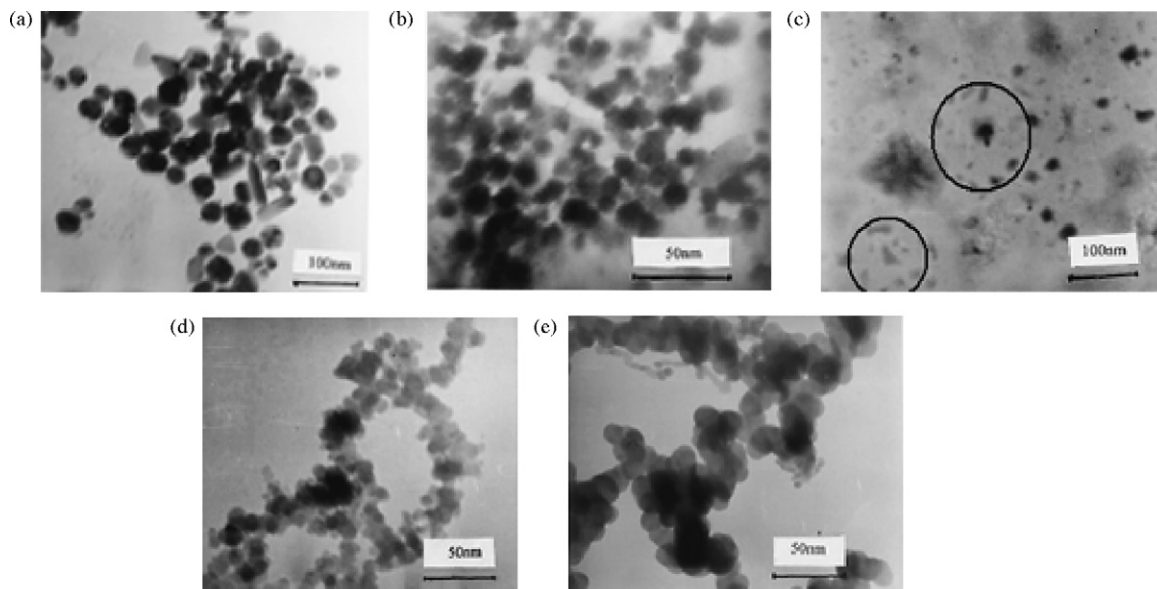


Fig. 2. Electron micrographs of silver nanoparticles (a); pure CdS (b); Ag–CdS nanocomposite containing different molar ratio of Ag to CdS: 0.1 (c); 0.25 (d); 1 (e).

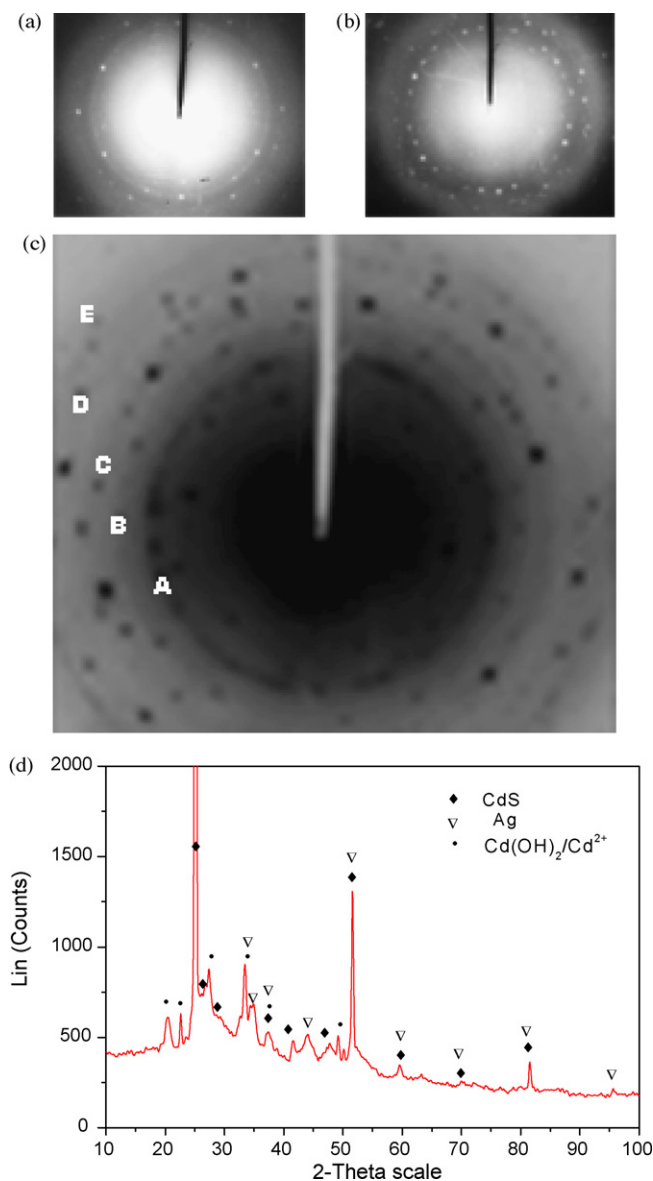


Fig. 3. Electron diffraction patterns of colloidal CdS (a); colloidal Ag (b); Ag–CdS nanocomposite (c)—indexing of its various diffraction patterns: (A) (1 1 0) of CdS with $d=2.06$ Å; (B) (0 0 6) of Ag, (0 0 4) of CdS with $d=1.67$ Å; (C) (1 1 2) of Ag, (2 1 0) of CdS with $d=1.38$ Å; (D) (2 0 3) of Ag, (3 0 0) of CdS with $d=1.17$ Å; (E) (0 0 1 0) of Ag with $d=1.00$ Å; (d) X-ray diffraction pattern of Ag–CdS nanocomposite containing molar ratio of Ag to CdS: 0.1.

the above findings from SAED pattern that both CdS and silver are present in hexagonal crystalline phase(s), respectively. Besides, some additional peaks due to free Cd^{2+} and formation of $\text{Cd}(\text{OH})_2$ were also noted.

It may be mentioned that some of the observed peaks due to Ag and CdS phases are in common to Acanthite phase of Ag_2S . These peaks had fairly low intensity, the peaks known to be having high intensity due to this phase were, however, missing. It thus rules out the formation of Ag_2S phase in these experiments.

The fluorescence spectra of pure CdS and Ag/CdS composites, having varied molar ratio of Ag to CdS keeping the amount of CdS constant, were recorded upon excitation by 340 as well

Table 1

Comparison of observed d -spacings (Å) in XRD pattern of Ag–CdS nanocomposite to those of standard values for hexagonal-CdS, hexagonal-Ag, and $\text{Cd}(\text{OH})_2$

Observed value	Hexagonal-CdS	Hexagonal-Ag	$\text{Cd}(\text{OH})_2/\text{Cd}^{2+}$ hex./mono
4.34	–	–	4.34
3.90	–	–	3.90
3.54	3.56	–	–
3.33	3.34	–	–
3.26	–	–	3.24 (mono)
3.15	3.15	–	–
2.58	–	2.50	2.54 (hex.)
2.40	2.44	2.42	2.41 (hex.)
2.16	–	–	2.16
2.05	2.06	–	–
2.01	–	2.00	–
1.90	1.89	–	–
1.85	–	–	1.85 (hex.)
1.76	1.75	1.76	–
1.54	1.57	1.56	–
1.34	1.35	1.38	–
1.17	1.19	1.17	–
1.03	–	1.02	–

as 420 nm light at pH 10.5 in the presence of air. The 340 nm light is largely absorbed by CdS phase as Ag nanoparticles have relatively negligible absorption at this wavelength, whereas at 420 nm both Ag and CdS phases absorbed light almost equally being having very similar extinction coefficient. The fluorescence spectra obtained upon excitation by 340 nm are shown in Fig. 4A. The used colloidal CdS solution depicts the low fluorescence intensity (curve a) in agreement to the literature data [22]. At lower molar ratios of Ag up to 0.25, the fluorescence intensity due to CdS is increased (curves b and c) along with a slight blue shift in the fluorescence maxima at low Ag (curve b). On the other hand at higher molar ratio, the fluorescence intensity is simply reduced without bringing any shift in its fluorescence maxima. At molar ratio of unity, the fluorescence intensity is significantly reduced and becomes smaller (curve e) than that of pure CdS particles. A very similar changes in emission behavior were noted when these particles were excited by 420 nm light except that the emission intensity were lower by a factor of about 1.6, which was equivalent to the ratio of molar absorptivity of Ag to CdS at this wavelength. Aging of these particles for overnight resulted in an enhancement of the emission intensity further by about 1.4-fold for each addition of Ag compared to that of freshly prepared CdS nanoparticles.

In order to check a possibility that at high pH the hydroxylation of the surface might be contributing to the observed effect on fluorescence behavior, the pH of the colloidal solution was varied from 8 to 11. It showed negligibly small changes in the emission characteristics, thus ruling out the contribution to the fluorescence due to surface modification through hydroxylation under the used experimental conditions. The possibility of involvement of O_2 was examined by performing fluorescence measurements under N_2 environment. It did not influence the fluorescence behavior in general except that the intensity of emission for initial additions of Ag was reduced but attained

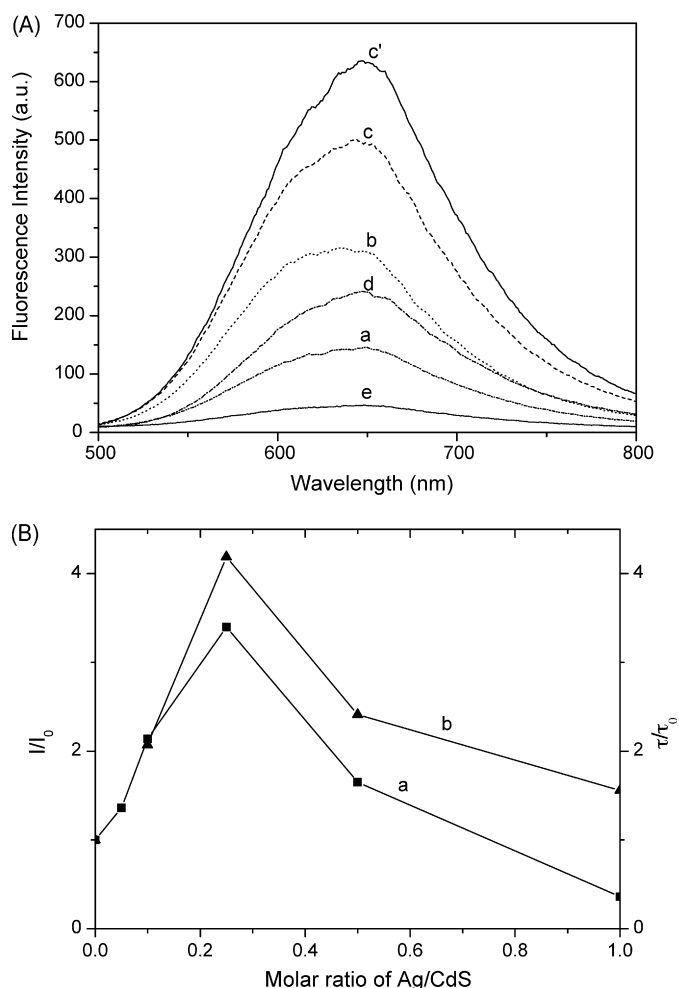


Fig. 4. (A) Emission spectra of Ag–CdS nanocomposite containing varied molar ratio of Ag to CdS: 0.0 (a); 0.1 (b); 0.25 (c); 0.5 (d); 1 (e); 0.25 (c', aged). (B) Plots of I/I_0 and τ/τ_0 as a function of molar ratio of Ag/CdS (curves a and b), respectively.

the maximum intensity, equivalent to that observed in the presence of air, at a little higher mole ratio of Ag:CdS. It may be mentioned that a simple mixing of the separately prepared two colloids behaved in a very similar fashion except the optical and emission changes noted in this case were of less magnitude compared to those when Ag was added prior to precipitation of CdS.

The complex variation in the intensity of emission as a function of added Ag was further analyzed by measuring the fluorescence lifetime under different experimental conditions (Fig. 5; Table 2). All the decay curves could be best fitted in three exponential kinetic programs consisting of three distinct ranges of sub-nanosecond, nanoseconds and tens of nanoseconds time domains. An increase in the molar ratio of Ag in Ag/CdS composite from 0.1 to 0.25 initially enhanced the average lifetime ($\langle\tau\rangle$) from 4.1 to 17.2 ns but it decreased significantly at high mol fractions of Ag. At unit molar ratio of Ag, $\langle\tau\rangle$ is reduced to 6.4 ns. Aging of various samples in general depicted an increase in $\langle\tau\rangle$ at all molar ratio of Ag (Table 2). The magnitude of increase was, however, not proportionate to the Ag content. At higher concentration of silver the lifetime is rather reduced abruptly. In

N₂ environment the fluorescence lifetime depicted a decrease in $\langle\tau\rangle$ for all the samples (not shown).

The photostability of these particles was studied by photolyzing different reaction samples by light of wavelength 340 ± 10 nm. An increase in the amount of silver up to molar ratio of 0.25 enhanced the quantum efficiency of photodegradation of CdS nanoparticles by a factor of 4 to that of in the absence of Ag, thereafter, an increase in silver, however, reduced it to become very similar to that of unmodified particles. In the N₂ environment the quantum efficiency of photodecomposition was about half to that of in the presence of air.

4. Discussion

The electronic spectral behavior and the electron micrographs of colloidal silver, CdS and their composites reveal a physical interaction between silver and CdS particles at both low and high concentrations of Ag (Figs. 1 and 2). At low molar ratios of silver to CdS the organization of silver and CdS phases is such that the silver and CdS particles are surrounded randomly by each other in which an interparticle distance was estimated to be 10–30 nm. At higher silver, clusters are formed and CdS particles are now present at the interface of Ag suggesting more intimate interaction between the two. The absence of any new phase in XRD clearly suggests the presence of two phases, which are possibly bound through weak van der Waals forces.

A decrease in absorption recorded upon mixing of silver and CdS phases might result due to damping of the electron oscillations in plasmon resonance because of the changed surrounding medium. This phenomenon become more prominent at high concentrations of silver where intimate interaction between the two is likely. A blue shift in its spectra compared to that of a simple sum spectra could possibly arise due to increased electron density on Ag by the injection of electron from the conduction band of CdS [23]. Colloidal silver particles have large double layer capacity, which might be charged cathodically by accepting electron, and thus lead to an increase in the electron density. The reverse process, i.e., an injection of electron from the excited Ag into CdS is ruled out from the steady-state fluorescence measurements in which the excitation of Ag–CdS composite by 420 nm radiation, which would excite the surface plasmon of Ag, did not exhibit any change in the emission behavior (vide infra).

An enhancement in the emission intensity at relatively low Ag and a reduction in its intensity at high Ag upon excitation of CdS particle demonstrate a complex steady-state emission behavior (Fig. 4A). The low amount of silver modifies the surface of CdS by binding to shallow as well as the deep traps involved in non-radiative transitions, which results in a slight blue shift in emission at fairly low Ag (curve b) along with an increase in the emission intensity of 650 nm band due to CdS nanoparticles upto about five-fold at mild Ag. The time resolved analysis of 650 nm fluorescence decay also demonstrates an increase in the percentage emission and the emission lifetime due to recombination of deeply trapped charge carriers lying in tens of nanosecond time domain (Table 2). It clearly suggests

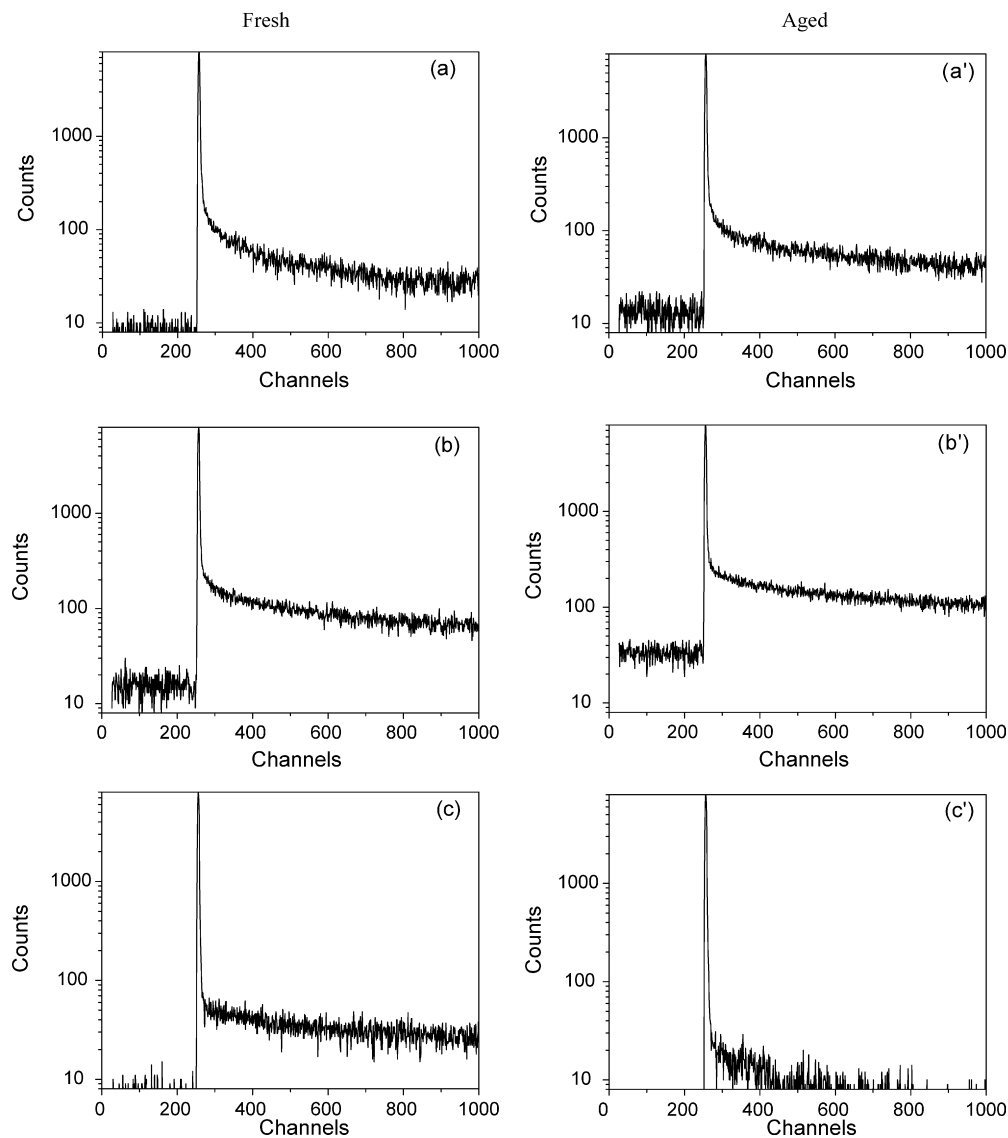


Fig. 5. Fluorescence decay curves of fresh and aged Ag–CdS nanocomposite containing different molar ratio of Ag to CdS: 0.0 (a, a'); 0.25 (b, b') 1 (c, c').

Table 2
Effect of variation in molar ratio of Ag/CdS on the lifetime of CdS

Molar ratio of Ag/CdS	Component 1		Component 2		Component 3		τ (ns)	χ^2
	τ_1 (ns)	Emission (%)	τ_2 (ns)	Emission (%)	τ_3 (ns)	Emission (%)		
(a) Fresh samples								
0.0	0.15 (3.63)	81.56	1.34 (2.93×10^{-2})	5.77	30.45 (2.84×10^{-3})	12.67	4.1	1.18
0.1	0.16 (3.16)	78.04	1.64 (1.41×10^{-2})	3.57	45.26 (2.64×10^{-3})	18.39	8.5	1.12
0.25	0.30 (3.16)	66.18	4.55 (8.47×10^{-3})	4.00	56.05 (5.13×10^{-3})	29.81	17.2	1.52
0.5	0.28 (2.06)	80.73	3.03 (3.27×10^{-3})	1.39	54.08 (2.36×10^{-3})	17.89	9.9	1.49
1.0	0.28 (2.07)	88.88	2.57 (1.27×10^{-3})	0.50	57.54 (1.21×10^{-3})	10.62	6.4	1.43
(b) Aged samples								
0.0	0.24 (2.09)	77.38	3.13 (8.79×10^{-3})	4.16	51.14 (2.39×10^{-3})	18.46	9.7	1.05
0.1	0.12 (5.01)	67.13	2.47 (1.29×10^{-2})	3.53	51.91 (5.11×10^{-3})	29.34	15.4	1.27
0.25	0.36 (2.82)	56.78	8.76 (7.31×10^{-3})	3.56	72.68 (9.80×10^{-3})	39.68	29.4	2.61
0.5	0.17 (3.08)	80.27	1.26 (1.90×10^{-2})	3.61	48.42 (2.22×10^{-3})	16.13	8.1	1.03
1.0	0.20 (2.55)	92.26	0.82 (2.56×10^{-2})	3.77	40.36 (5.50×10^{-4})	3.97	1.8	1.38

$\lambda_{\text{ex}} = 340 \text{ nm}$; $\lambda_{\text{em}} = 650 \text{ nm}$.

function of [Ag] (Fig. 4A and B, Table 2). Such a correlation in the steady-state intensity and the lifetime is in accordance to the classical theory of fluorescence [30]. This observation is though different with the previously studied Ag/CdTe system [19] in which the presence of Ag enhances the fluorescence intensity of CdTe accompanied with a decrease in its lifetime. Further, these observations have been made with CdTe coated on silver island films, which may be quite different as regard to the [Ag] and its interaction with CdTe in thin film compared to those employed in the present work. In the presence of air, CT complex (CdS (h^+) . . . Ag $^-$) decomposes partially by transferring electron to O₂ (Eq. 2), which eventually results in the photodecomposition of CdS (vide ut supra). Such photoinduced electron transfer is expected to occur more efficiently at higher Ag because of the intimate contact between CdS and Ag (Fig. 2d and e). The observation that at low Ag hole corrodes CdS more efficiently whereas at high Ag its photodecomposition is reduced, it can be understood by the fact that under the latter conditions Ag surrounds CdS effectively which does not allow hole to escape and recombines with the plasmon electron in a non-radiative process. The efficient quenching of emission and a drastic reduction in $\langle\tau\rangle$ under these conditions also supports this hypothesis (Figs. 4 and 5).

Thus at low Ag an increase in the fluorescence intensity of CdS is contributed by the formation of relatively long-lived CT complex whereas at higher Ag this complex is decomposed as shown in Eq. 3 by shifting the equilibrium in the forward direction. Under these conditions CdS is present at the interface of Ag (Fig. 2), which causes the electron transfer from the CT complex to become rapid to result in the quenching of emission and a reduction in emission lifetime. The extent of electron transfer in this intermediate is controlled kinetically as per Eqs. (1)–(3). The observation that in experiments conducted under N₂/inert environment a little higher amount of Ag is required to obtain a similar enhancement in the intensity of CdS (vide ut supra), it can be understood by the formation of CT complex at relatively slower rate (Eq. (4)) as compared to in the presence of air which drives the equilibrium in the forward direction (Eq. (2)).

In summary the addition of Ag to CdS modifies its surface, which influences the optical and fluorescence behavior of CdS in the composite. The extent of Ag affects the interparticle separation. A low molar ratio of Ag induces the fluorescence whereas the high amount of Ag quenches its emission. These changes are understood due to the formation of transitory CT complex between CdS* and Ag, which is destabilized at high Ag due to rapid electron transfer from the excited CdS into the Ag phase. This study provides an insight into the mechanism of interparticle interaction and dynamics of their charge carriers. Such systems could be useful in designing of devices for luminescence and photocatalytic work.

Acknowledgements

The financial support of DST, New Delhi is gratefully acknowledged to undertake this work. VC is thankful to DST & MHRD, New Delhi for the award of JRF. Thanks are also due to the Head, IIC, IITR, Roorkee for providing us the facilities of XRD, Single Photon counter and TEM.

References

- [1] M.-C. Daniel, D. Astruc, *Chem. Rev.* 104 (2004) 293.
- [2] C.D. Grant, T.J. Norman Jr., J.Z. Zhang, in: H.S. Nalwa (Ed.), *Encyclopedia of Nanoscience and Nanotechnology*, vol. 1, 2004, p. 745.
- [3] P.V. Kamat, *Pure Appl. Chem.* 74 (2002) 1693.
- [4] A.P. Alivisatos, *J. Phys. Chem.* 100 (1996) 13226.
- [5] J. Yang, H.I. Elim, Q. Zhang, J.Y. Lee, W. Ji, *J. Am. Chem. Soc.* 128 (2006) 11921.
- [6] T. Mokari, E. Rothenberg, I. Popov, R. Costi, U. Banin, *Science* 304 (2004) 1787.
- [7] G.H. Ma, J. He, K. Rajiv, S.H. Tang, Y. Yang, M. Nogami, *Appl. Phys. Lett.* 84 (2004) 4684.
- [8] J. Lee, A.O. Govorov, J. Dulka, N.A. Kotov, *Nano Lett.* 4 (2004) 2323.
- [9] H.S. Zhou, I. Honma, J.W. Haus, H. Sasabe, H. Komiyama, *J. Lumin.* 70 (1996) 21.
- [10] Y. Wang, M. Li, H. Jia, W. Song, X. Han, J. Zhang, B. Yang, W. Xu, B. Zhao, *Spectrochim. Acta, Part A* 64 (2006) 101.
- [11] S. Zou, M.J. Weaver, *Chem. Phys. Lett.* 312 (1999) 101.
- [12] I. Honma, T. Sano, H. Komiyama, *J. Phys. Chem.* 97 (1993) 6692.
- [13] F. Rocco, A.K. Jain, M. Treguer, T. Cardinal, S. Yatte, P.L. Coustumer, C.Y. Lee, S.H. Park, J.G. Chai, *Chem. Phys. Lett.* 394 (2004) 324.
- [14] J. Belloni, M. Mostafavi, H. Remita, J.-L. Marignier, M.-O. Delcourt, *New J. Chem.* 22 (1998) 1239.
- [15] H.Y. Lin, Y.F. Chen, J.G. Wu, D.I. Wang, C.C. Chen, *Appl. Phys. Lett.* 88 (2006) 161911.
- [16] B. Pal, T. Torimoto, K. Iwasaki, T. Shibayama, H. Takahashi, B. Ohtani, *J. Electrochem.* 35 (2005) 751.
- [17] J. Kolny, A. Kornowski, H. Weller, *Nano Lett.* 2 (2002) 361.
- [18] P.V. Kamat, B. Shanghavi, *J. Phys. Chem. B* 101 (1997) 7675.
- [19] K. Ray, R. Badugu, J.R. Lakowicz, *J. Am. Chem. Soc.* 128 (2006) 8998.
- [20] J. Turkevich, P.C. Stevenson, Hiller, *J. Discuss. Faraday Soc.* 11 (1951) 55.
- [21] Z.S. Pillai, P.V. Kamat, *J. Phys. Chem.* 108 (2004) 945.
- [22] (a) A. Kumar, S. Kumar, *J. Photochem. Photobiol. A: Chem.* 69 (1992) 91; (b) N. Gupta, M. Phil. Dissertation, Dept. of Chemistry, IITR, Roorkee, India, 2003.
- [23] P. Mulvaney, *Langmuir* 12 (1996) 788.
- [24] A. Kumar, S. Kumar, *Chem. Lett.* (1996) 711.
- [25] (a) In a blank experiment Ag₂S was produced by varying the amount of Ag⁺ (5×10^{-7} to 2×10^{-6} mol dm⁻³) to CdS (1×10^{-4} mol dm⁻³), these particles exhibited an onset of absorption at 2.37 eV; (b) To the above prepared Ag₂S particles, different amounts of Ag⁺ (5×10^{-7} to 2×10^{-6} mol dm⁻³) were added to Ag/CdS nanocomposites having a molar ratio of 0.1. Even very small amount of Ag⁺ ($\leq 1 \times 10^{-6}$ mol dm⁻³) resulted in the quenching of emission due to CdS.
- [26] A. Kumar, A.K. Jain, *J. Photochem. Photobiol. A: Chem.* 156 (2003) 207.
- [27] T. Ung, M. Giersig, D. Dunstan, P. Mulvaney, *Langmuir* 13 (1997) 1773.
- [28] A. Henglein, *Ber. Bunsenges. Phys. Chem.* 86 (1982) 301.
- [29] K. Mallick, M. Witcomb, M. Scurrill, *Mater. Chem. Phys.* 97 (2006) 283.
- [30] J.R. Lakowicz, *Principles of Fluorescence Spectroscopy*, 2nd ed., Kluwer Academic/Plenum Publishers, New York, 1999, p. 14.